Biosensors and Bioelectronics 91 (2017) 400–407

Contents lists available at ScienceDirect

Biosensors and Bioelectronics

journal homepage: www.elsevier.com/locate/bios

G-quadruplex-based fluorometric biosensor for label-free and homogenous detection of protein acetylation-related enzymes activities

Huixia Wang[a,1], Yong Li[a,1], Kunli Zhao[a], Siyi Chen[a], Qin Wang[a], Bin Lin[b,c,*], Zhou Nie[a,**], Shouzhuo Yao[a]

[a] State Key laboratory of Chemo/Biosensing and Chemometrics, College of Chemistry and Chemical Engineering, Hunan University, Changsha 410082, People's Republic of China

[b] Department of Medicinal Chemistry, School of Pharmaceutical Engineering, Shenyang Pharmaceutical University, Shenyang 110016, People's Republic of China

[c] Key Laboratory of Structure-Based Drug Design & Discovery, Ministry of Education, Shenyang Pharmaceutical University, Shenyang 110016, People's Republic of China

ARTICLE INFO

Keywords:
Histone acetyltransferases
Histone deacetylases
G-quadruplexes
Thioflavin T
Label-free fluorescent method

ABSTRACT

Reversible protein acetylation, one of the key types of post-translational modifications, is composed of histone acetylation and deacetylation, which is typically catalyzed by histone acetyltransferases (HATs) and histone deacetylases (HDACs) respectively. Herein, a label-free fluorescent method has been established for the homogeneous bioassay of HAT/HDAC activity and respective inhibitors. The proposed approach is primarily based on the electrostatic interaction between G-quadruplexes (G4s) and acetylation-related peptides, which results in marked change of fluorescent intensity of G4/Thioflavin T (ThT) complexes. This HAT (p300) activity assay is exceedingly sensitive and selective, with a linear range from 0.1 to 120 nM and a detection limit of 0.05 nM. Moreover, this biosensor is feasible to detect the HDAC (Sirt1) activity with a linear range from 1 to 450 nM and a detection limit of 1 nM. The potency of this assay is further demonstrated by detecting HAT/HDAC activity in cell lysates and evaluating HAT and HDAC-targeted inhibitors, C464 and EX 527, respectively. The proposed assay is convenient, label-free and cost-efficient, which is promising for HAT/HDAC-targeted epigenetic research and pharmaceutical development.

1. Introduction

Histone modification, a covalent post-translational modification (PTM) to histone proteins, is of vital importance in epigenetic regulation (Strahl and Allis, 2000; Zhang et al., 2015). Owing to the histone modification, diverse biological events such as transcriptional activation/inactivation, chromosome packaging, and DNA damage/repair can be controllably carried out (Biel et al., 2005; Zhao et al., 2010; Wang et al., 2010). Particularly, reversible acetylation on lysine residues is one of the major mechanisms of histone modification. The level of histone lysine acetylation is accurately mediated by the antagonistic catalytic activity of histone acetyltransferases (HATs) and histone deacetylases (HDACs) (Jenuwein and Allis, 2001; Seligson et al., 2005). Through acetylation, HAT reduces electrostatic interactions between histones and their wrapping DNA, producing an open chromatin structure for the accessibility of regulatory proteins. In contrast, HDAC catalyzes acetyl group removal and enhances the linkage of histones and genes, leading to a closed chromosomal configuration and transcriptional repression. Aberrant activity of HAT or HDAC, inducing the disturbance of histone acetylation, has been validated relevant to the etiology of numerous diseases, including cancer, neurological disorders, chronic inflammation, and HIV infection (Dekker and Haisma, 2009). To date, HAT/HDAC has emerged as a novel class of drug targets and HAT/HDAC-targeted inhibitors are also under extensive investigation. To expedite such investigation, the development of convenient assay methods of HAT/HDAC activity is urgently required, which is significant in drug development and pharmaceutical studies of clinical diagnosis, and is also essential for better understanding of epigenetics-related research.

Traditional methods for monitoring the activity of HAT/HDAC are

* Corresponding author at: Department of Medicinal Chemistry, School of Pharmaceutical Engineering, Shenyang Pharmaceutical University, Shenyang 110016, People's Republic of China.

** Corresponding author.

E-mail addresses: randybinlin@gmail.com (B. Lin), niezhou.hnu@gmail.com (Z. Nie).

[1] These two authors contributed equally to this work.

http://dx.doi.org/10.1016/j.bios.2016.12.065
Received 16 October 2016; Received in revised form 2 December 2016; Accepted 29 December 2016
Available online 30 December 2016
0956-5663/

based on acetyl-lysine-specific antibodies, such as western blot, enzyme-linked immunosorbent assay (ELISA), colorimetric and fluorescent assay kits of acetyl-specific antibodies (Kuninger et al., 2007; Zhen et al., 2012). Generally, these methods suffer from the intrinsic drawbacks of antibodies, such as low stability, high batch-to-batch variability, and high cost. Alternative methods for antibody-free assays have also been developed, *e.g.*, antibody-free assays *via* recognition of acetylated products, detection based on inhibition of protease degradation or acetylation-induced peptide regulation on nano-materials (Chen et al., 2015; Hu et al., 2015; Han et al., 2015). Though above antibody-free methods have simplified the operations to some extent, some complicated steps, such as covalent labeling of peptides with fluorochromes, treatment with expensive toolkit of enzymes, or requirement of costly instruments, are still necessary during detection processes (Li et al., 2016a, 2016b). Therefore, more endeavors are needed to develop a novel antibody-free method for facile, low-cost, robust and homogenous bioassay of such enzymes. Moreover, a detection platform of high-throughput screening and evaluation of HAT/HDAC-targeted inhibitors is preferable for pharmacological and therapeutic purposes.

Recently, functional nucleic acids of G-quadruplexes (G4s) have attracted great interest as versatile molecular toolkits (Kong et al., 2010; Jin et al., 2013; Qi et al., 2013; Huang et al., 2014). In general, G4s are unique four-stranded nucleic acid structures which are formed by stacking of Hoogsteen base paired G-quartets, and this phenomenon is prevalent in G-rich sequences (Parkinson et al., 2002; Li et al., 2016a, 2016b). Interestingly, thioflavin T (ThT) was recently demonstrated to be highly specific for G4s, and its binding with G4s causes a striking fluorescence light-up in the visible region (Mohanty et al., 2012). In addition, the fluorescigenic G4/ThT complexes have been widely investigated as fluorescent probe due to their impressive advantages of low cost, facility, strong stability, high signal-to-background, and quick signal response. To date, the G4/ThT-based sensors have already been implemented for various detections of DNA-related analytes, such as biomarkers of ions, microRNAs, DNA-relevant nuclease, and ligands of aptamers (Ruttkay-Nedecky et al., 2013; Liu et al., 2014). However, to the best of our knowledge, G4-based bioassays have not been applied to detections of histone acetylation-related enzymes. Since the electrostatic interactions between histone and DNA are reversibly controlled by the acetylation/deacetylation-related enzymes, it is intriguing to develop a sensing mechanism for HAT/HDAC activity which mimics the interaction between histones and DNA mediated by protein acetylation. Hence, we envisioned that a G4/ThT-based probe could be exploited for homogeneous detection of acetylation and acetylation-related enzymes activity.

In this research, a label-free fluorescent biosensor was developed for sensitive detection of acetylation-related enzymes activity of HAT and HDAC. It was established in virtue of the interaction between G4-DNA and acetylated-substrate peptide, and the fluorescence emission of G4/ThT complexes. Similar to acetylation-mediated histone-DNA interaction, the charge change caused by lysine-acetylation of substrate peptides leads to the different competitiveness between peptides and ThT to bind G4, displaying a significant difference in fluorescent intensity. Through monitoring the G4/ThT-emitted fluorescence, the HAT-mediated acetylation process and the HDAC-mediated deacetylation process were homogenously detected, respectively. Compared with the conventional HAT/HDAC sensing methods, the proposed fluorometric biosensor presents a new sensing platform for probing HAT and HDAC activity, which overcomes common shortcomings including sophisticated peptide labeling, time-consuming, low sensitivity, and intricate sensing mechanism. Moreover, the sensing platform provides a robust protocol for high-throughput screening and evaluation of HAT/HDAC-targeted inhibitors, holding great potential in epigenetic research and drug discovery.

2. Experimental section

2.1. Materials and reagents

Single-strand DNA (ssDNA) used in this work were synthesized and purified by Sangon Inc. (Shanghai, China). The sequences of ssDNA are listed in Table S1. Sirtuin1 (Sirt1) HDAC, p300 HAT, β-nicotinamide adenine dinucleotide hydrate (NAD^+), acetyl coenzyme A (Ac-CoA), C646, thioflavin T (ThT), lysozyme, bovine serum albumin (BSA), horseradish peroxidase (HRP), glucose oxidase (GOx), protein kinase A (PKA), acetylcholinesterase (AChE) and caspase-3 (Caspase) were purchased from Sigma-Aldrich (Shanghai, China). EX 527 was purchased from Selleck (Shanghai, China). Substrate peptide P(+) (RGKGGKGLGKGGAKA) and acetylated peptide P(Ac) (RGK(Ac)GGK(Ac)GLGK(Ac)GGAK(Ac)A) were purchased from Aite peptide Ltd. (Nanjing, China). All solutions were prepared with ultrapure water (18.2 MΩ·cm, 25 °C) from the Millipore Milli-Q system.

2.2. Apparatus

The fluorescence measurements for detecting HAT (p300) and HDAC (Sirt1) inhibitors were collected by a Synergy Mx multimode microplate reader (BioTek, USA). All other fluorescence spectra were surveyed on the Quanta Master™ 4 fluorescence spectrometer (PTI, Canada). The circular dichroism (CD) spectra were performed on a MOS-500 spectrophotometer (BioLogic, France). The hydrodynamic diameter was recorded by dynamic light scattering (DLS, UK). The hydrogel imaging results were collected by Gel Doc XR System (Bio-Rad, USA).

2.3. Detection of HAT (p300) activity and its inhibitor

For HAT p300 activity, p300 at various concentrations (from 0 to 400 nM) was incubated with substrate peptide P(+) (10 μM) and Ac-CoA (100 μM) in borate buffer (10 mM, pH 7.5) with a total volume of 10 μL for 90 min at 30 °C. After the enzyme reaction, TBA (100 nM) was injected in and incubated for 30 min at 30 °C, followed by adding ThT (4 μM) and a certain volume of ultrapure water (final sample volume 100 μL). After incubation for 1 min, the fluorescence of the mixture solutions were measured. For HAT p300 inhibition, p300 (120 nM), substrate peptide P(+) (10 μM), and p300 inhibitor C646 at different concentrations (from 0 to 60 μM) were pre-incubated for 10 min at room temperature in borate buffer (10 mM, pH 7.5). After that the reaction was initiated by the addition of Ac-CoA (100 μM) with a total volume of 10 μL at 30 °C for 90 min, and then the rest of the steps were the same as in the detection of p300 activity.

2.4. Detection of HDAC (Sirt1) activity and its inhibitor

For HDAC Sirt1 activity, Sirt1 at various concentrations (from 0 to 600 nM) was incubated with acetylated peptide P(Ac) (10 μM) and NAD^+(200 μM) in borate buffer (10 mM, pH 7.5) with a total volume of 10 μL at 30 °C for 80 min. After the enzyme reaction, TBA (100 nM) was injected in and incubated for 30 min at 30 °C, followed by adding ThT (4 μM) and a certain volume of ultrapure water (final sample volume 100 μL). After incubation for 1 min, the fluorescence of the mixture solutions were measured. For Sirt1 inhibition, Sirt1 (400 nM), acetylated peptide P(Ac) (10 μM), and Sirt1 inhibitor EX 527 at different concentrations (from 0 to 10 μM) were pre-incubated for 10 min at room temperature in borate buffer (10 mM, pH 7.5). After that the reaction was initiated by the addition of NAD^+(200 μM) with a total volume of 10 μL at 30 °C for 80 min, and then the rest of the steps were the same as the detection of Sirt1 activity.

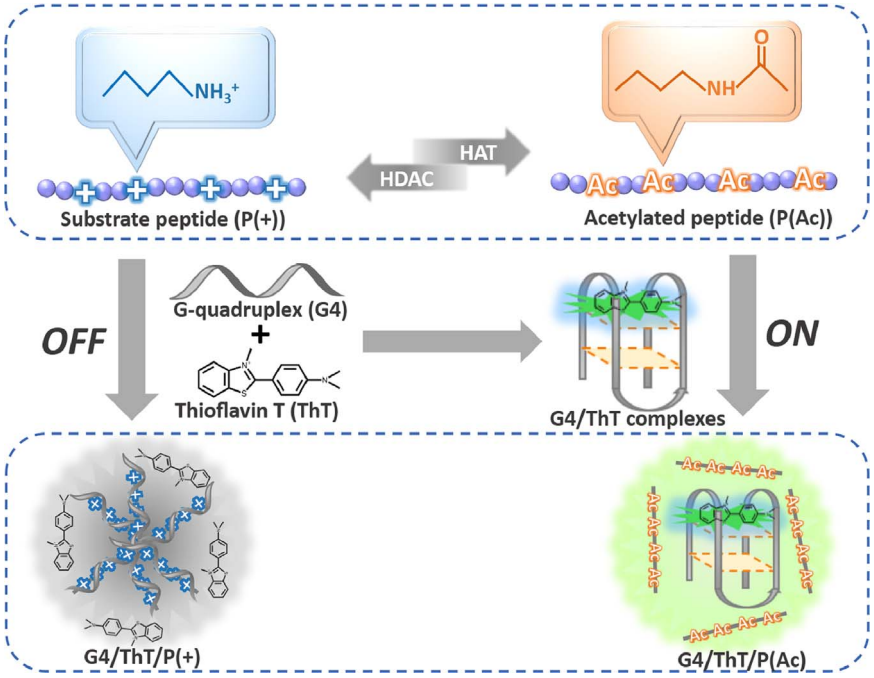

Scheme 1. Schematic illustration of fluorescent assay of histone acetyltransferases (HATs) and histone deacetylases (HDACs) activity.

3. Results and discussion

3.1. The principle of detection of HAT and HADC

The principle of developing a label-free fluorescence biosensor for probing HAT and HAT activity is schematically illustrated in Scheme 1. The G-rich DNA sequence can be folded into a G-quadruplex structure with thioflavin T (ThT) as inducer, resulting in a great enhancement of ThT fluorescence intensity in the visible light region (Mohanty et al., 2012). The fluorescence signal of ThT dye is employed as the output signal of the proposed assay. The 15 amino acids (aa)-long substrate peptide P(+) carries four positively charged lysine residues which is derived from the H4 N-terminal histone tail. The positively charged substrate peptides interact with G4s to form a stable peptide/G4 complexes, preventing the formation of G4/ThT and producing little fluorescent emission. After acetylation by HAT, the positive charges from the substrate peptide P(+) are significantly removed, causing the dissociation of peptide/G4 complexes. The newly released G4 recombine with ThT, resulting in the fluorescent signal recovery. Similarly, the addition of HDAC removed the acetyl group of P(AC) and generated the positively charged P(+), inducing the fluorescent signal of G4/ThT off. By this mean, the “OFF” or “ON” of G4/ThT-based fluorescent switch is reversibly controlled by HAT or HDAC. Through monitoring the fluorescent emission variation, a homogenous bioassay for HAT/HDAC activities could be achieved.

3.2. Discrimination of acetylated peptide and substrate peptide by the proposed assay

To achieve optimal performance of the proposed assay, the experimental conditions were systematically investigated. The fluorescence emission spectra at different experimental conditions were recorded, and the value of F_a/F_b (F_a/F_b is the fluorescence intensity ratio of G4/ThT coexisting with P(Ac) (F_a) and P(+) (F_b) respectively) was used to assess the effects of the experimental conditions on the performance of the proposed assay. Initially, 11 kinds of G-rich DNA sequence were investigated. As illustrated in Fig. 1A, all the G4-DNA structures could discriminate the acetylated peptide and substrate peptide, and three of them, including 17DNA, thrombin-binding aptamer (TBA) and mutPu22, showed a better performance ($F_a/F_b > 500\%$). In addition, the 15-base TBA with two stack G-quartets in borate buffer had the best performance than 17DNA and mutPu22 (Fig. S1A). After that, the concentrations of the reactants for the assay were optimized to be 100 nM TBA, 4 μM (ThT) and 1 μM (peptides) (Fig. S2 and S3). The other reaction conditions of TBA/ThT used in the assay were optimized to be two-steps (reaction approaches), 30 °C (temperature) and 30 min (reaction time) (Fig. S4, S5 and S6).

Under the optimized experimental conditions, a series of characterization experiments were carried out to investigate the discrimination of TBA/ThT on the acetylated peptide and substrate peptide. Visualization hydrogel imaging of different addition of TBA, ThT, P(+) and P(Ac) is shown in Fig. 1B. The fluorescence of hydrogel spots of ThT and TBA/ThT/P(+) are relatively weak, while those of TBA/ThT and TBA/ThT/P(Ac) are much stronger. The corresponding normalized fluorescence intensity is shown in Fig. 1C. TBA, ThT and TBA/ThT/P(+) have almost no fluorescence signal, but the fluorescence signals of TBA/ThT and TBA/ThT/P(Ac) are markedly enhanced. These results sufficiently indicated that the acetylated peptide and substrate peptide could be discriminated by the fluorescence intensity of TBA/ThT. Moreover, the structural change of TBA was investigated by the circular dichroism (CD) spectra. As shown in Fig. 1D, the unfolded TBA has weak positive bands around 255 and 285 nm, as well as weak trough ~265 nm (Zhao et al., 2014). Upon addition of ThT, a positive band at ~265 nm and a negative band at ~240 nm appear. The results prove that the formation of parallel G4 structures, which is consistent with the previous report (Mohanty et al., 2012). After the incubation of P(Ac) with TBA/ThT complexes, the peak value at ~265 nm is nearly unchanged, indicating the complexes are intact. However, the peak value is decreased significantly at ~265 nm with the incubation of P(+) with TBA/ThT complexes, indicating the TBA/ThT complexes are destroyed by the stronger electrostatic interaction between P(+) and TBA. Furthermore, the average hydrodynamic radius of TBA/P(+) complexes was investigated. As shown in Fig. S7, an average hydrodynamic radius of 195 ± 69 nm is characterized by dynamic light scattering (DLS), confirming the formation of the TBA/P(+) complexes. Therefore, the above evidence proves that the acetylated peptide and

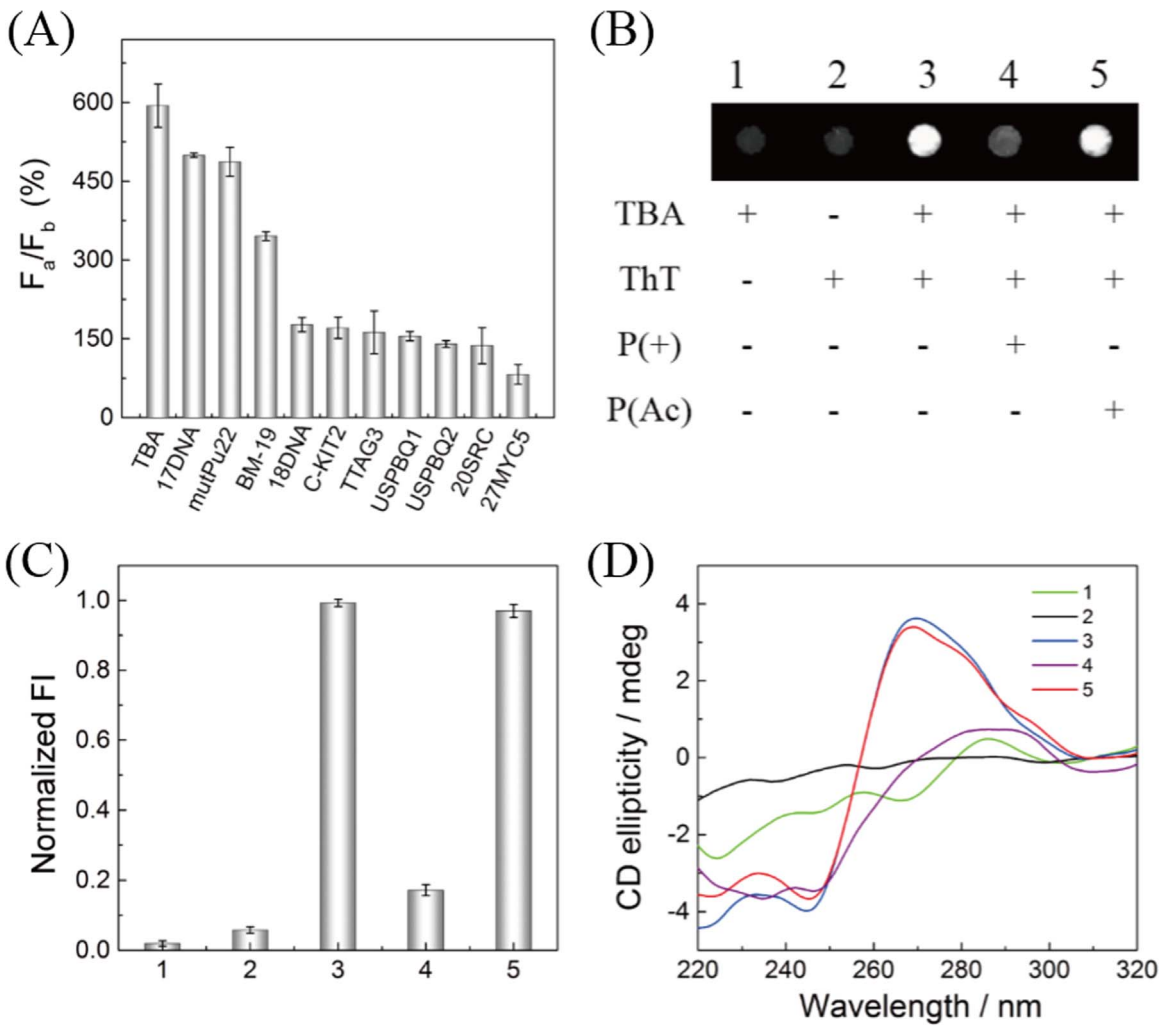

Fig. 1. (A) Optimization experiments for the sequence of G4s (the sequences of ssDNA are listed in Table S1). The hydrogel image (B), the normalized fluorescence intensity (λ_{ex}=425 nm) (C), and the circular dichroism spectra of TBA (1), ThT (2), TBA/ThT (3), TBA/ThT/P(+) (4) and TBA/ThT/P(Ac) (5). Noted that F_a/F_b is the fluorescence intensity ratio of TBA/ThT coexisting with P(Ac) (F_a) and P(+) (F_b) respectively. [G4s]=100 nM, [ThT]=4 μM, [P(+)]=1 μM, [P(Ac)]=1 μM.

substrate peptide could be readily discriminated by the proposed assay.

3.3. Analytical performance of the HAT biosensor

The p300 protein, an important member of HAT family, activates transcription *via* binding to transcription factors and is involved in the complex biological processes that affect cell growth, development and transformation (Goodman and Smolik, 2000). The p300 protein catalytically transfers the acetyl functional group from the acetyl-coenzyme A (Ac-CoA) to the specific lysine residues within the N-terminus of the core histone proteins. Therefore, p300 was chosen as the model HAT enzyme for the activity assay. In Fig. 2A, it demonstrates that the fluorescence intensity presents about 85% enhancement after the addition of p300, whereas the control samples, including P(+), the coexistence of p300 and P(+), and the coexistence of Ac-CoA and P(+) show rare fluorescence emission. In addition, the p300, the Ac-CoA, and the coexistence of p300 and Ac-CoA have no influence on the fluorescence intensity of TBA/ThT complexes (Fig. S8). These results clearly suggest that the activity of p300 can be detected by the proposed assay.

To examine the selectivity of the proposed HAT biosensor, some different non-specific proteins, including lysozyme, bovine serum albumin (BSA), horseradish peroxidase (HRP), glucose oxidase (GOx), protein kinase A (PKA), acetylcholinesterase (AChE), caspase-3 (Caspase) were selected to challenge the HAT biosensors. As displayed in Fig. 2B, the presence of p300 leads to a significant fluorescent response, while the presence of non-specific proteins has negligible effects on the fluorescent signal compared to the blank test (in the absence of p300). Moreover, the effect of co-existing of the above non-specific proteins on the detection of p300 was investigated. The results shown in the inset of Fig. 2B prove that the co-existence of each above non-specific proteins hardly interferes with the proposed HAT biosensor. It clearly indicates that the HAT biosensor facilely discriminates between p300 and the non-specific proteins with high specificity.

For sensing performance analysis, it was evaluated by quantitative detection of p300 activity at various concentrations. The fluorescence intensity upon addition of different concentration of p300 was recorded. Fig. 3A displays the typical fluorescence emission signals of the proposed sensing system corresponding to a series of different concentrations of p300. It is observed that the fluorescence emission intensity gradually increases when the concentration of p300 is elevated from 0 to 600 nM. There is a good liner relationship between the fluorescence intensity and the p300 concentration in the range of 0.1–120 nM, as shown in Fig. 3B. The linear regression equation is $Y=0.00637\times C_{p300}+0.152$ ($R^2=0.995$). Thus, it is demonstrated that the p300 activity can be quantitatively analyzed by the plot of fluorescence intensity *versus* enzyme concentrations. The limit of detection (LOD) is found to be 0.05 nM (S/N=3), which is better than most of the other developed approaches. The detailed comparison of these p300 activity is listed in Table S2.

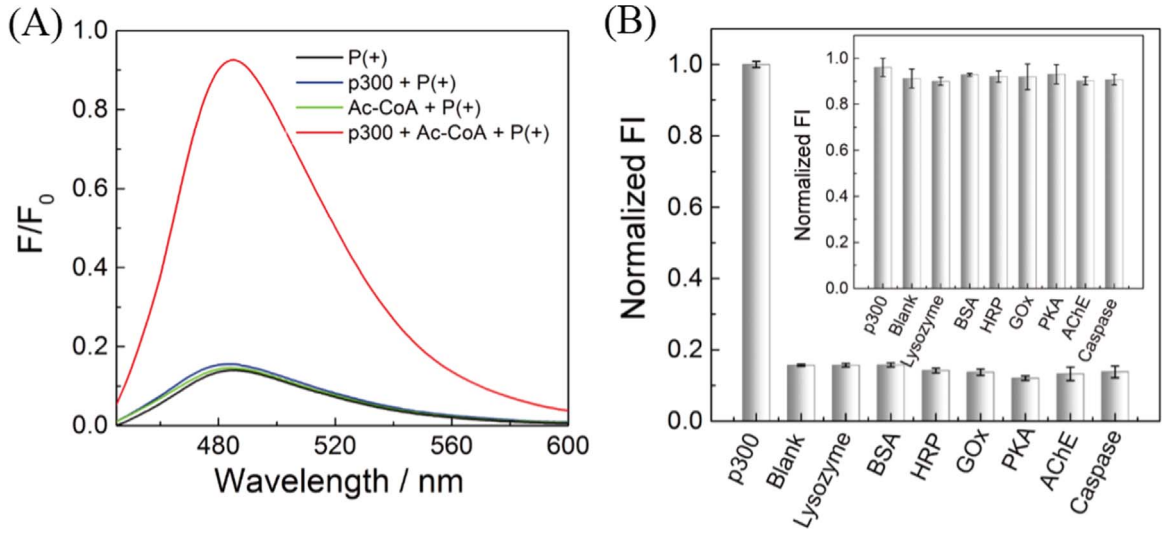

Fig. 2. (A) Response of the HAT biosensor to P(+), p300/P(+), Ac-CoA/P(+), and p300/Ac-CoA/P(+). (B) The bar graph corresponding to the selective experiment of the HAT biosensor. The HAT-catalyzed reaction ([p300]=120 nM) was conducted in the absence (Blank) or presence of different non-specific proteins (120 nM) including lysozyme, bovine serum albumin (BSA), horseradish peroxidase (HRP), glucose oxidase (GOx), protein kinase A (PKA), acetylcholinesterase (AChE) and caspase-3 (Caspase). Inset in (B) is the fluorescence responses of the proposed assay of p300 and p300 co-existed with different non-specific proteins. F/F_0 is the fluorescence intensity ratio of the proposed assay and TBA/ThT complexes.

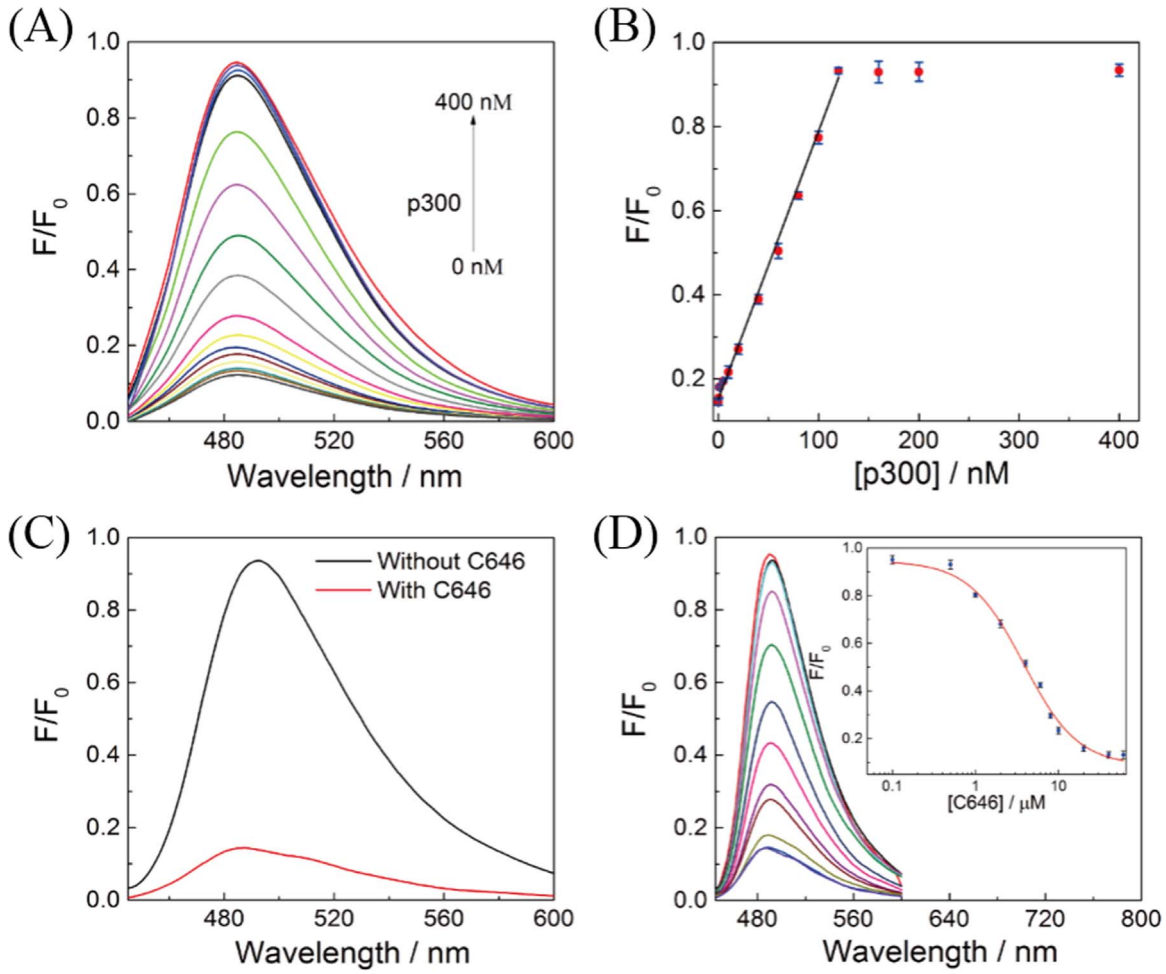

Fig. 3. (A) The fluorescence spectra of the HAT assay responsive to increasing concentrations of p300 (from bottom to top: 0, 0.05, 0.1, 0.5, 1.0, 5.0, 10, 20, 40, 60, 80, 100, 100, 120, 160, 200 and 400 nM) and (B) its calibration curve. (C) The fluorescence spectra of the HAT assay in response to the absence (black line) and presence (red line) of 60 μM p300 inhibitor C646. (D) Various concentrations of C646 were used for p300 inhibition. From top to bottom ([C646]: 0, 0.1, 0.5, 1.0, 2.0, 4.0, 6.0, 8.0, 10, 20, 40 and 60 μM). Inset in (D) shows the fluorescence signal curve as a function of the concentration of C646. [p300]=120 nM. (For interpretation of the references to color in this figure legend, the reader is referred to the web version of this article.)

Besides selectivity and sensitivity, the detection of p300 assay in complex samples is also significant for exploiting the potential of the proposed assay in practical applications. Thus, a recovery experiment was performed by addition of different concentrations of p300 into the HeLa cell lysates. The HeLa cell lysates were treated by DNase I and RNase to remove cellular DNA and RNA. The detection results corresponding to p300 in the 10,000 cells/mL HeLa cell lysates were basically consistent with those under the buffer conditions. As illustrated in Table S3, the recoveries vary from 99% to 103% and the relative standard deviation (RSD) is below 3.5%, demonstrating the potential of the HAT biosensor for HAT (p300) activity detection in real biological samples.

3.4. Investigation on HAT inhibitors based on the HAT biosensor

HAT inhibitors are potential drugs for the treatment of several related diseases, such as inflammatory diseases, cancers and psychological disorders. Therefore, a sensitive assay for screening inhibitors of HAT enzyme is vital for drug development. A potent small-molecule inhibitor, C646, is a competitive inhibitor of p300 that antagonizes Ac-CoA, and it was shown to suppress histone acetylation in human cells *in vitro*. It was chosen to test its inhibitory activity to p300 detected by the HAT biosensor (Bowers et al., 2010). Fig. 3C demonstrates the feasibility of the inhibition experiment. The fluorescence intensity decreases about 84.7% with the addition of 60 μM C646. Furthermore, the HAT biosensor is able to measure the inhibitory activity quantitatively by exposing p300 to a series of dilutions of C646. As shown in Fig. 3D, the fluorescent signal decreases gradually with increasing concentration of C646, elucidating its inhibitory ability of C646. The dose-response curve for C646 is sigmoidal (the inset of Fig. 3D) and the IC_{50} value of C646 toward p300 is estimated to be 3.78 ± 0.42 μM, well consistent with the literature values (Bowers et al., 2010). These results suggest that the HAT biosensor can be applicable for screening HAT inhibitors.

3.5. Analytical performance of the HDAC biosensor

As members of Class III histone deacetylases (HDACs), sirtuins act primarily by removing acetyl groups from N-acetyl-lysine residues within histone proteins in the presence of nicotinamide adenine dinucleotide (NAD^+). Sirtuin1 (Sirt1) is a member of the sirtuin family that contributes to cellular regulation and is involved in metabolism and age-related diseases (Longo and Kennedy, 2006). In this work, Sirt1 was chosen as a model HDAC enzyme. For feasibility analysis, as shown in Fig. 4A, the fluorescence intensity of the reaction of P(Ac) with Sirt1 and the co-substrate NAD^+ is markedly decreased compared with the control samples, including P(Ac), the coexistence of Sirt1 and NAD^+, and the coexistence of NAD^+ and P(Ac). The results indicate that the acetyl groups on lysines are removed, thus quenching the fluroscence signal of the assay. Addition of Sirt1-specific inhibitor (EX 527) (Gertz et al., 2013) completely inhibits the fluorescence decreases, indicating that the HDAC-catalyzed deacetylation causes a significant fluorescence signal change. In addition, the Sirt1, the NAD^+, or the coexistence of Sirt1 and NAD^+ have no influence on the fluorescence intensity of TBA/ThT complexes (Fig. S9). These results clearly demonstrate that the activity of Sirt1 can be detected by the proposed assay.

Selectivity is an important factor that determines the performance and utilization of the HDAC biosensor. Thus the selectivity of the HDAC biosensor was explored by substituting Sirt1 with several different non-specific proteins, namely lysozyme, bovine serum albumin (BSA), horseradish peroxidase (HRP), glucose oxidase (GOx), protein kinase A (PKA), acetylcholinesterase (AChE) and caspase-3 (Caspase). As shown in Fig. 4B, none of these non-specific proteins turns off the fluorescence of the ThT dye. Moreover, the effect of co-existing of the above non-specific proteins on the detection of Sirt1 was also investigated (see Fig. S10). These results fully prove that the co-existence of each above-mentioned non-specific protein does not interfere with the proposed HDAC biosensor. Furthermore, these results clearly indicate the high selectivity of the proposed strategy for HDAC (Sirt1) activity over other interfering proteins, which can facilitate the practical application of HDAC (Sirt1) in complex samples.

The analytical performance of the developed strategy for Sirt1 HDAC activity detection was examined. The fluorescence intensity upon the addition of different concentration of Sirt1 was recorded. According to Fig. 4C, the fluorescence intensity of ThT dye decreases gradually with the increasing concentrations of Sirt1 from 0 to 600 nM. The inset of Fig. 4C shows that there is a good linearity between the fluorescence intensity at 485 nm of the HDAC assay and Sirt1 concentration in the range of 1–450 nM. The linear regression equations is $Y=-0.00176\times C_{Sirt1}+0.932$ ($R^2=0.992$). The LOD for Sirt1 is 1 nM (S/N=3). In addition, the analytical performance of the proposed HDAC biosensor was superior or comparable to the previously reported methods for sirt1 detection (detailed comparison shown in Table S2).

To test the potential application of the proposed strategy to a complex sample, we employed the HeLa cell lysates as model matrix. The HeLa cell lysates were treated by DNase I and RNase to remove cellular DNA and RNA. Recovery experiment was performed by adding various concentrations of Sirt1 to HeLa cell lysates to test the accuracy of the proposed method. The detection results corresponding to Sirt1 in the 10,000 cells/mL HeLa cell lysates were basically consistent with those under buffer conditions. The quantitative results were summarized in Table S4, with the recoveries varying from 98% to 106% and the RSD below 5.5%. These results are consistent with those for Sirt1 detection in buffer solutions, further confirming the biosensor for HDAC (Sirt1) activity detection is promising for the detection of Sirt1 activity in real biological samples.

3.6. Investigation on HDAC inhibitors based on the HDAC biosensor

Sirtuins are considered as promising targets for drug discovery and the screening of its inhibitors can provide potential drugs for related diseases, including metabolic diseases, cancer, and age-related diseases. Hence, the HDAC biosensor was further employed for quantitative screening of the inhibitor for the Sirt1. EX 527 was chosen as a model compound because it is a potent and specific small-molecule Sirt1 inhibitor and was used in many physiological studies. The inhibitory effects of EX 527 on Sirt1 activity were examined using the proposed assay. Fig. 4D depicted the fluorescence spectral responses in the presence of EX 527 at varying concentrations. The fluorescence emission peaks were observed to increase dynamically with the increasing EX 527 concentration in the range from 5 nM to 10 μM. The fluorescence emission at 485 nm displayed a sigmoid correlation to the concentrations of EX 527, and the IC_{50} value of EX 527 toward Sirt1 was estimated to be 0.079 ± 0.034 μM, in good accordance with the literature values (the inset of Fig. 4D) (Gertz et al., 2013). These findings demonstrate that the proposed Sirt1 activity assay can be successfully applied in Sirt1 inhibitor screening and is a potentially useful tool for drug discovery.

3.7. Evaluation of the proposed assay for high-throughput screening HAT/HDAC inhibitors

Developing a high-throughput screening (HTS) assay is very important for accurately and rapidly identify HAT/HDAC inhibitors and determining its IC_{50} values. To demonstrate the ability of the HAT/HDAC biosensors for high-throughput screening of HAT/HDAC inhibitors, we use a coefficient called “Z′-factor”. The value of Z′-factor should be within the range of 0.5 and 1.0 to show a wide separation of positive and negative results (Zhang et al., 1999). As shown in Fig. 5A and B, the Z′-factors of C646 and EX 527 were 0.71 and 0.68,

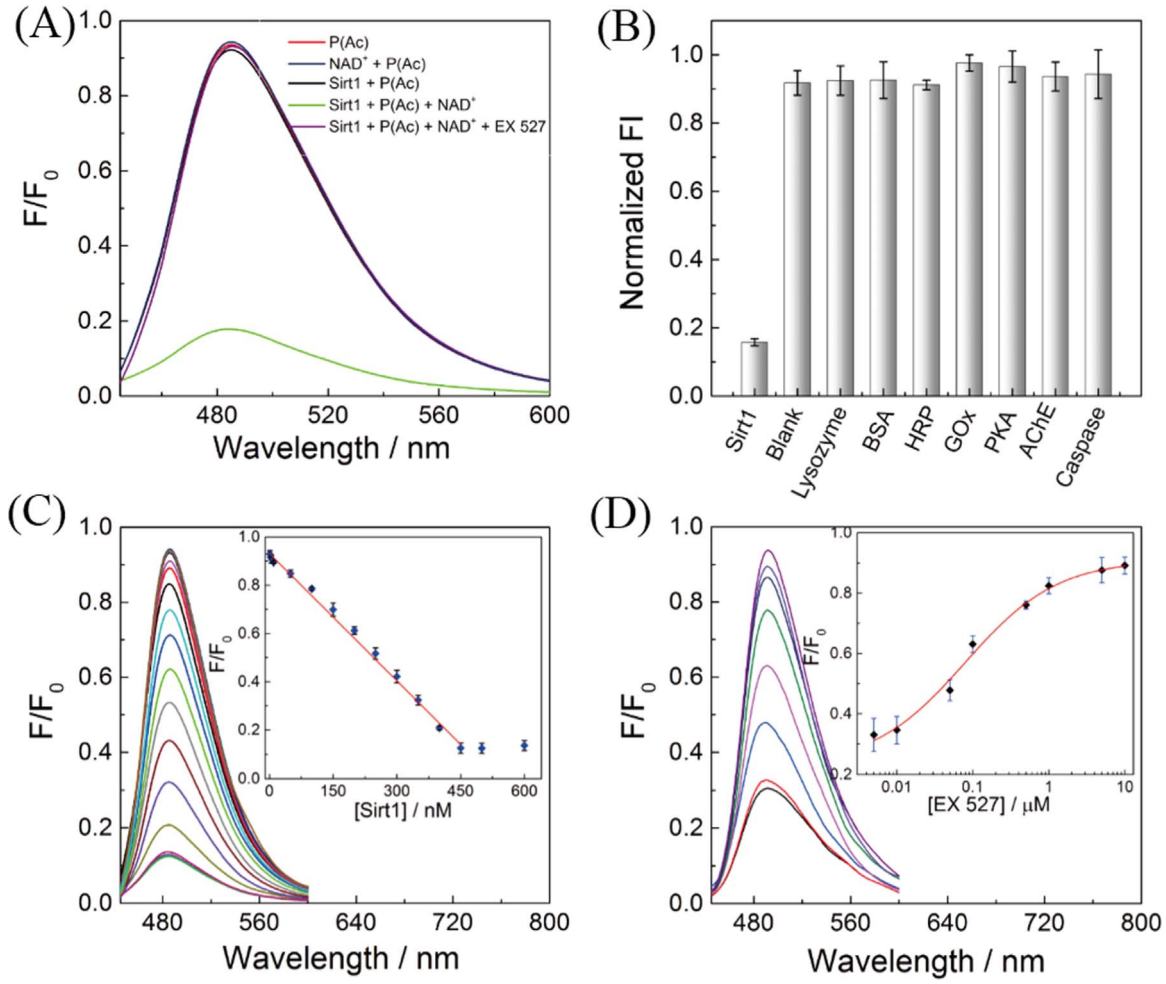

Fig. 4. (A) Response of the HDAC biosensor to P(Ac), Sirt1/P(Ac), NAD^+/P(Ac), Sirt1/P(Ac)/NAD^+, and Sirt1/P(Ac)/NAD^+/EX 527. (B) The bar graph corresponding to the selective experiment of the HDAC biosensor. The HDAC-catalyzed reaction ([Sirt1]=400 nM) was conducted in the absence (Blank) or presence of different non-specific proteins (400 nM). (C) The fluorescence spectra of the HDAC assay responsive to increasing concentration of Sirt1 (from top to bottom: 0, 0.5, 1.0, 5.0, 10, 50, 100, 150, 200, 250, 300, 350, 400, 450, 500 and 600 nM) and its calibration curve (inset). (D) Various concentrations of HDAC Sirt1 inhibitor EX 527 were used for HDAC inhibition. From bottom to top ([EX 527]: 0, 0.005, 0.01, 0.05, 0.1, 0.5, 1, 5 and 10 μM). Inset in (D) shows the fluorescence signal curve as a function of the concentration of EX 527 ([Sirt1]=350 nM).

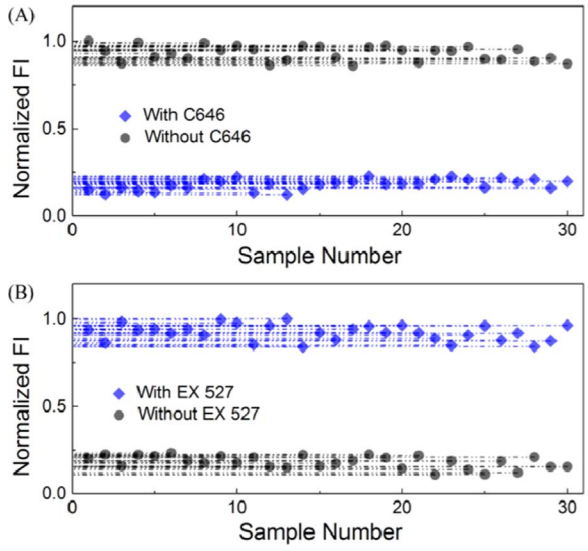

Fig. 5. The evaluation of the proposed assay for high-throughput screening of 60 μM C646 (A) and 10 μM EX527 (B).

respectively, demonstrating that the proposed assay would be a robust strategy with good reproducibility for HTS.

4. Conclusions

In summary, we developed a label-free fluorescent biosensor for sensitive and specific monitoring the acetylation-related enzymes HAT/HDAC activity and screening its inhibitors. To the best of our knowledge, this work demonstrated for the first time that the interaction between G4 and acetylation-relation peptides could be applied to assay the activity and inhibition of HAT/HDAC. The results revealed that this method was implemented conveniently through homogeneous reactions and enabled the detection in a robust manner. Moreover, it works for enzymes activity assay in practical samples, such as cell lysates. Compared with traditional methods, our proposed method presents several advantages: (i) our assay is label-free and avoids sophisticated chemical modification; (ii) it shows good analytical performance, such as wide detection range, high sensitivity and selectivity; (iii) it is facile, convenient and time-saving, which can be exploited for the high-throughput screening of HAT/HDAC inhibitors; (iv) all reagents in this assay are commercially available and cost-efficient. We expect that our strategy could be a promising sensing platform for HAT/HDAC-related epigenetic research and HAT/HDAC-targeted drug screening.

Acknowledgement

This work was financially supported by the National Natural Science Foundation of China (Nos. 21235002 and 21575038), the Foundation for Innovative Research Groups of NSFC (Grant 21521063), and the Natural Science Foundation of Hunan Province (No. 2015JJ1005).

Appendix A. Supporting information

Supplementary data associated with this article can be found in the online version at doi:10.1016/j.bios.2016.12.065.

References

Biel, M., Wascholowski, V., Giannis, A., 2005. Angew. Chem. Int. Ed. 44, 3186–3216.
Bowers, E.M., Yan, G., Mukherjee, C., Orry, A., Wang, L., Holbert, M.A., Crump, N.T., Hazzalin, C.A., Liszczak, G., Yuan, H., Larocca, C., Saldanha, S.A., Abagyan, R., Sun, Y., Meyers, D.J., Marmorstein, R., Mahadevan, L., Alani, R.M., Cole, P.A., 2010. Chem. Biol. 17, 471–482.
Chen, S., Li, Y., Hu, Y., Han, Y., Huang, Y., Nie, Z., Yao, S., 2015. Chem. Commun. 51, 4469–4473.
Dekker, F.J., Haisma, H.J., 2009. Drug Discov. Today 14, 942–948.
Gertz, M., Fischer, F., Nguyen, G.T.T., Lakshminarasimhan, M., Schutkowski, M., Weyand, M., Steegborn, C., 2013. Proc. Natl. Acad. Sci. USA 110, E2772–E2781.
Goodman, R.H., Smolik, S., 2000. Gene. Dev. 14, 1553–1577.
Han, Y., Li, P., Xu, Y., Li, H., Song, Z., Nie, Z., Chen, Z., Yao, S., 2015. Small 11, 877–885.
Hu, Y., Chen, S., Han, Y., Chen, H., Wang, Q., Nie, Z., Huang, Y., Yao, S., 2015. Chem. Commun. 51, 17611–17614.
Huang, X.X., Zhu, L.N., Wu, B., Huo, Y., Duan, N., Kong, D., 2014. Nucleic Acids Res. 15, 8719–8731.
Jenuwein, T., Allis, C.D., 2001. Science 293, 1074–1080.
Jin, B., Zhang, X., Zheng, W., Liu, X., Qi, C., Wang, F., Shangguan, D., 2013. Anal. Chem. 1, 943–952.
Kong, D.M., Xu, J., Shen, H.X., 2010. Anal. Chem. 14, 6148–6153.
Kuninger, D., Lundblad, J., Semirale, A., Rotwein, P., 2007. J. Biotechnol. 131, 253–260.
Li, P., Han, Y., Li, Y., Zhu, Y., Wang, H., Nie, Z., Yao, S., 2016a. Anal. Bioanal. Chem. 11, 2659–2668.
Li, W., Li, Y., Liu, Z., Lin, B., Yi, H., Xu, F., Nie, Z., Yao, S., 2016b. Nucleic Acids Res. 15, 7373–7384.
Liu, Z., Li, W., Nie, Z., Peng, F., Huang, Y., Yao, S., 2014. Chem. Commun. 52, 6875–6878.
Longo, V.D., Kennedy, B.K., 2006. Cell 126, 257–268.
Mohanty, J., Barooah, N., Dhamodharan, V., Harikrishna, S., Pradeepkumar, P.I., Bhasikuttan, A.C., 2012. J. Am. Chem. Soc. 135, 367–376.
Parkinson, G.N., Lee, M.P.H., Neidle, S., 2002. Nature 417, 876–880.
Qi, C., Bing, T., Mei, H., Yang, X., Liu, X., Shangguan, D., 2013. Biosens. Bioelectron. 41, 157–162.
Ruttkay-Nedecky, B., Kudr, J., Nejdl, L., Maskova, D., Kizek, R., Adam, V., 2013. Molecules 18, 14760–14779.
Seligson, D.B., Horvath, S., Shi, T., Yu, H., Tze, S., Grunstein, M., Kurdistani, S.K., 2005. Nature 435, 1262–1266.
Strahl, B.D., Allis, C.D., 2000. Nature 403, 41–45.
Wang, Q., Zhang, Y., Yang, C., Xiong, H., Lin, Y., Yao, J., Li, H., Xie, L., Zhao, W., Yao, Y., Ning, Z., Zeng, R., Xiong, Y., Guan, K., Zhao, S., Zhao, G., 2010. Science 327, 1004–1007.
Zhang, J.H., Chung, T.D.Y., Oldenburg, K.R., 1999. J. Biomol. Screen. 4, 67–73.
Zhang, X., Liu, C., Wang, H., Wang, H., Li, Z., 2015. Angew. Chem. Int. Ed. 50, 15186–15190.
Zhao, D., Dong, X., Jiang, N., Zhang, D., Liu, C., 2014. Nucleic Acids Res. 42, 11612–11621.
Zhao, S., Xu, W., Jiang, W., Yu, W., Lin, Y., Zhang, T., Yao, J., Zhou, Li, Zeng, Y., Li, H., Li, Y., Shi, J., An, W., Hancock, S.M., He, F., Qin, L., Chin, J., Yang, P., Chen, X., Lei, Q., Xiong, Y., Guan, K., 2010. Science 327, 1000–1004.
Zhen, Z., Tang, L., Long, H., Jiang, J., 2012. Anal. Chem. 84, 3614–3620.